

N-Methyldihydroquinazolinone Derivatives of Retro-2 with Enhanced Efficacy against Shiga Toxin

Romain Noel,[†] Neetu Gupta,[‡] Valérie Pons,[†] Amélie Goudet,[‡] Maria Daniela Garcia-Castillo,[§] Aurélien Michau,[‡] Jennifer Martinez,[‡] David-Alexandre Buisson,[†] Ludger Johannes,[§] Daniel Gillet,^{*,‡} Julien Barbier,[‡] and Jean-Christophe Cintrat^{*,†}

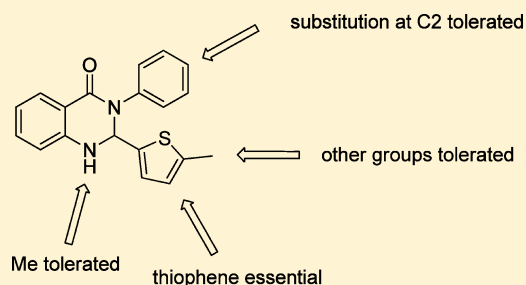
[†]CEA, iBiTec-S/SCBM, CEA-Saclay, LabEx LERMIT, F-91191 Gif-sur-Yvette, France

[‡]CEA, iBiTec-S/SIMOPRO, CEA-Saclay, LabEx LERMIT, F-91191 Gif-sur-Yvette, France

[§]UMR144 CNRS and Traffic, Signaling, and Delivery Laboratory, Institut Curie, 26 Rue d'Ulm, 75248 Paris Cedex 05, France

Supporting Information

ABSTRACT: The Retro-2 molecule protects cells against Shiga toxins by specifically blocking retrograde transport from early endosomes to the trans-Golgi network. A SAR study has been carried out to identify more potent compounds. Cyclization and modifications of Retro-2 led to a compound with roughly 100-fold improvement of the EC₅₀ against Shiga toxin cytotoxicity measured in a cell protein synthesis assay. We also demonstrated that only one enantiomer of the dihydroquinazolinone reported herein is bioactive.



INTRODUCTION

The Shiga toxin (Stx) family consists of a number of structurally and functionally related protein toxins that are mainly produced by the bacteria *Shigella dysenteriae* and certain strains of *E. coli*.^{1,2} Bacteria producing these toxins are pathogenic to humans and responsible for a number of diseases such as diarrhea, hemorrhagic colitis, and the life-threatening complication hemolytic uremic syndrome (HUS).³ The Stx-producing *E. coli* (STEC) strains, which cause these clinical manifestations, are designated as enterohemorrhagic *E. coli* (EHEC). Recently, a major outbreak, caused by the pathogenic *E. coli* O104:H4, occurred in central Europe during late spring of 2011, infecting nearly 4000 people mainly in Germany, causing more than 900 cases of HUS resulting in 54 deaths.⁴

Stx is a known potent inhibitor of protein biosynthesis in eukaryotic cells. After binding to its globotriaosylceramide (Gb3) receptor by nature of its B-subunit (STxB), Stx is internalized by endocytosis and navigates through the retrograde pathway from the plasma membrane to the endoplasmic reticulum (ER) via early endosomes and Golgi network.^{5,6} Once in ER, the enzymatic subunit (STxA) translocates to the cytosol and inactivates ribosomes, leading to a blockade in protein synthesis.

So far, no effective therapy exists for Stx intoxication. Management consists of early dialysis for acute renal failure and general supportive care. Plasma exchange has been tried without clear evidence of its efficacy and remains controversial in regard to HUS.^{7,8} However, the unprecedented epidemic of *E. coli* in 2011 served as an opportunity to evaluate on a large scale the beneficial effect of others drugs, such as the monoclonal antibody eculizumab directed against the comple-

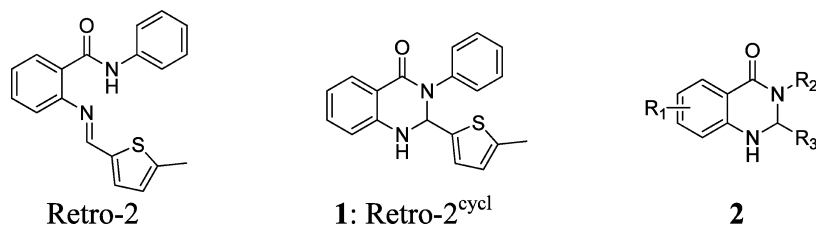
ment cascade and approved for the treatment of the genetic related disorder atypical HUS (aHUS). Indeed, an article published during the 2011 *E. coli* outbreak reported the successful treatment of three 3-year-old patients with severe STEC-HUS with eculizumab.⁹ Yet in a recent retrospective study no short-term benefit for adult cases of HUS was detected that could be attributed to the treatment with this antibody.⁸

In order to block the deleterious action of Stx, blockade of intracellular retrograde trafficking can be an option, as it has been recently demonstrated with small molecules.^{10–13} Most of these compounds have been identified by high throughput screening (HTS), but even after the first round of optimization they showed no therapeutic value mainly because of toxicity or poor inhibition activity. Very recently Mukhopadhyay and Linstedt reported on the use of large concentrations of manganese to block intracellular trafficking.¹⁴ Although Mn²⁺ based treatment holds therapeutic promise, the mandatory high doses (500 μM) seem to hinder clinical development. On the basis of a HTS, we recently identified that the compound Retro-2 was able to selectively block Stx retrograde trafficking at the early endosome–trans Golgi network (TGN) interface, hence protecting cells from the cytotoxic action of the toxins.¹¹ Unlike other toxin inhibitors, Retro-2 did not perturb cellular morphology nor did it affect other trafficking pathways. Here, we report on the development of a related compound Retro-2^{cycl} with a similar mode of action and improved protection efficacy for cells against Stx.

Received: February 14, 2013

Published: March 21, 2013

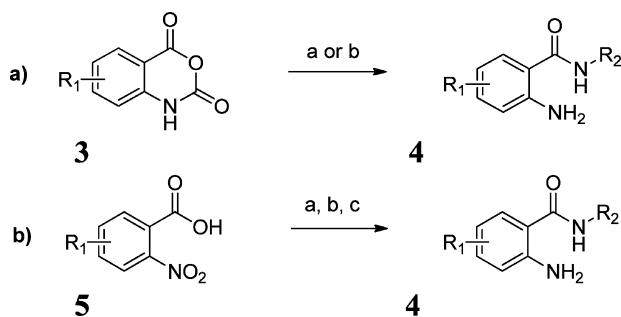
Scheme 1



CHEMISTRY

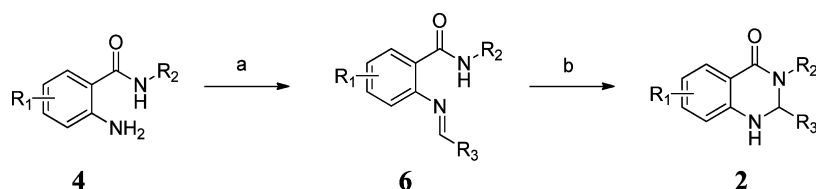
During the course of our SAR process, we discovered that the bioactive compound was not Retro-2 but the cyclized analogue Retro-2^{cycl} (Scheme 1). This finding has been recently published by Park et al.¹⁵ We therefore focused our attention towards the chemical optimization of Retro-2^{cycl} **1**, which indeed was a good starting point for optimization with three main sites available for diversity screening (R_1 , R_2 , and R_3 in Scheme 1). We evaluated individually the impact of R_1 , R_2 , R_3 and combined the best pharmacophores at the end, instead of a linear approach where R_3 would be optimized from the best R_2 , which itself was optimized from the best R_1 .

The general strategy for the synthesis of the dihydroquinazolinones of type **2** consisted of the formation of 2-aminobenzamide derivatives **4** (Scheme 2) followed by condensation of the resulting primary amine with aldehydes yielding the expected imino moiety **6** (Scheme 3).

Scheme 2^a

^aReagents and conditions. For reaction a: (a) R_2-NH_2 , neat, 130 °C, 2 h or (b) R_2-NH_2 , AcOH, reflux, 4 h. For reaction b: (a) $SOCl_2$, DCM, reflux, 2 h; (b) R_2-NH_2 , DCM, rt, 24 h; (c) H_2 , Pd/C, EtOAc, rt, 16 h.

Thus, the 2-aminobenzamide derivatives **4** were prepared as shown in Scheme 2 in two ways depending on the commercial availability of starting materials. First, isatoic anhydrides (compounds **3**) reacted with various amines in order to get 2-aminobenzamides **4** (Scheme 2, route a). Second, 2-nitrobenzoic acids were activated by $SOCl_2$ in DCM and the resulting acyl chlorides were reacted with various amines in

Scheme 3^a

^aReagents and conditions: (a) R_3CHO , MeOH, 16 h; (b) NaH, THF, 0 °C to rt, 16 h.

order to get 2-nitrobenzamides that were then hydrogenated to get the desired compounds **4** (Scheme 2, route b).¹⁸

The required imines were prepared as shown in Scheme 3. The resulting primary aromatic amines were condensed with aldehyde in methanol at room temperature, affording imines **6** in good yields. The expected cyclized compounds belonging to the dihydroquinazolinone family are easily obtained by cyclization with sodium hydride.

Since at the beginning of this SAR study we had compounds of general formula **6** in hand, we also screened the imino compounds. All compounds of general formula **6** showed similar or lower activities compared to the dihydroquinazolinones analogues (data not shown).

Three-component condensation of an isatoic anhydride, a primary amine, and an aldehyde has been widely described under a variety of catalysts to obtain dihydroquinazolinones,¹⁷ but in many cases, we experienced the formation of oxidized compounds. For instance, oxidized compound **7** was obtained under Brønsted conditions and exhibited no protection against Stx (Figure 1).

From the synthetic scheme, the last component to be involved in the synthesis of Retro-2^{cycl} was the aldehyde. In order to construct a library of analogues, we therefore focused attention on the impact of R_3 substituents on bioactivity.

All compounds synthesized using this scheme and the corresponding cell protection factor (see Experimental Section) are summarized in Table 1. A cell-based assay was used to detect the activity of Stx by measuring protein synthesis inhibition in eukaryotic cells and thus quantify the potency of inhibitors of toxin activity. In the first round of experiments, compounds were assayed at a fixed concentration of 30 μM on cells with increasing concentrations of Stx. Retro-2^{cycl} was used as a positive control to calculate the protection factor (see Experimental Section). Half-maximal effective concentrations, EC_{50} values, were only assessed for compounds displaying an activity equal to or better than **1**, i.e., a protection factor of >100%, as the EC_{50} value is more precise and robust to estimate a drug's potency.

From Table 1, it is clear that all the aromatic or heteroaromatic aldehydes tested (**8–13**) resulted in lower activity against Stx than the parent compound. The only pharmacophore that was allowed was substituted thiophene.

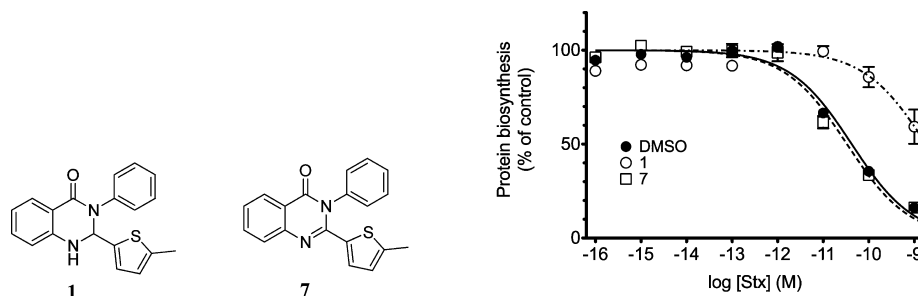


Figure 1. Effect of compound **1** and oxidized analogue **7** on cell protection against Stx. HeLa cells were incubated 4 h with **1** (open circles), **7** (open squares, dashed line), or carrier only (DMSO, black-filled circles) before addition of Stx at the indicated concentrations for 20 h. Medium was removed and replaced with DMEM containing [^{14}C]leucine at 0.5 $\mu\text{Ci}/\text{mL}$ for 6 h before counting. Each data point represents the mean of quadruplicate \pm SEM of a representative experiment.

Table 1. Analogues of Retro-2^{cycl}: R₃ Modifications^a

Compound	R ₃	Yield (%)	Protection factor (%)	EC ₅₀ (μM)	Compound	R ₃	Yield (%)	Protection factor (%)	EC ₅₀ (μM)
1			100	27.3	16		65	1	N.D.
8		84	0	N.D.	17		77	166	8.7
9		88	0	N.D.	18		77	54	N.D.
10		78	10	N.D.	19		91	146	13.7
11		77	48	N.D.	20		54	249	7.8
12		78	0	N.D.	21		74	287	3.7
13		84	0	N.D.	22		67	111.6	5.1
14		78	0	N.D.	23		61	468	12.0
15		85	0	N.D.	24		56	438	4.0
					25		42	271	1.40

^aN.D.: not determined.

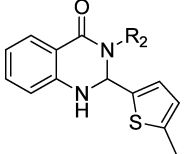
We were rather surprised to experience no activity with the unsubstituted thiophene **14**. Similarly 3-methyl- and 4-methylthiophene were inactive (**15**, **16**). Since it unambiguously appeared that the 5-position was the sole position that could be engaged in modification, we synthesized 5-substituted thiophene analogues of Retro-2^{cycl}.

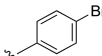
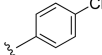
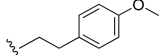
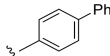
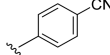
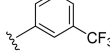
While the replacement of the methyl group (compound **1**) by an ethyl group resulted in higher protection (**17**, EC₅₀ = 8.7 μM), introduction of a propyl group (**18**) displayed only a modest activity. Elongation of the alkyl chain had a significant influence on activity. A slight improvement was also observed

with 5-Br and 5-thiomethyl analogues (**19** and **20**, EC₅₀ = 13.7 and 7.8 μM , respectively).

Importantly, introduction of small aromatic (**21**) or heteroaromatic groups (2-thiophene, 2-pyridine, 2-furyl, or 4-(2-methylthiazole)) demonstrated greater protection values when compared to the parent compound **1**. Finally the best compound in this series was **25**, displaying a 2-methyl, 1,3-thiazole tail with an EC₅₀ of 1.5 μM .

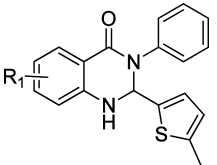
In a second round of SAR we then checked the influence of the substituent R₂.

Table 2. Exploration of R₂ Impact on Bioactivity


Compound	R ₂	Yield (%)	Protection Factor (%)	EC ₅₀ (μM)	Compound	R ₂	Yield (%)	Protection Factor (%)	EC ₅₀ (μM)
26		43	0	N.D.	38		52	0	N.D.
27	Bn	48	0	N.D.	39		29	0.5	N.D.
28		32	0	N.D.	40		56	0	N.D.
29		47	0	N.D.	41		65	0	N.D.
30		54	0	N.D.	42		10	0	N.D.
31		51	0	N.D.	43		60	0	N.D.
32		69	0	N.D.	44		58	54	N.D.
33		41	0	N.D.	45		17	211	14.8
34		20	0	N.D.	46		26	75	N.D.
35		59	0	N.D.					
36		50	0	N.D.					
37		29	0	N.D.					

Among all the substituents only the *o*-Cl **45** improved the bioactivity of the initial compound with R₂ = phenyl. Finally, a few analogues were synthesized to check for opportunities of structural variation at R₁ (Table 3).

Among the five compounds that we tested, the only improvement was seen with the 4-fluoro compound (com-

Table 3. SAR Exploration of R₁ in Analogues of Retro-2^{cycl} ^a


compd	R ₁	yield (%)	protection factor (%)	EC ₅₀ (μM)
47	5-Me	99	4	ND
48	4-Me	68	11.2	ND
49	4-MeO	71 ^b	2	ND
50	4-F	62 ^b	167.2	10.6
51	5-F	23 ^b	0	ND

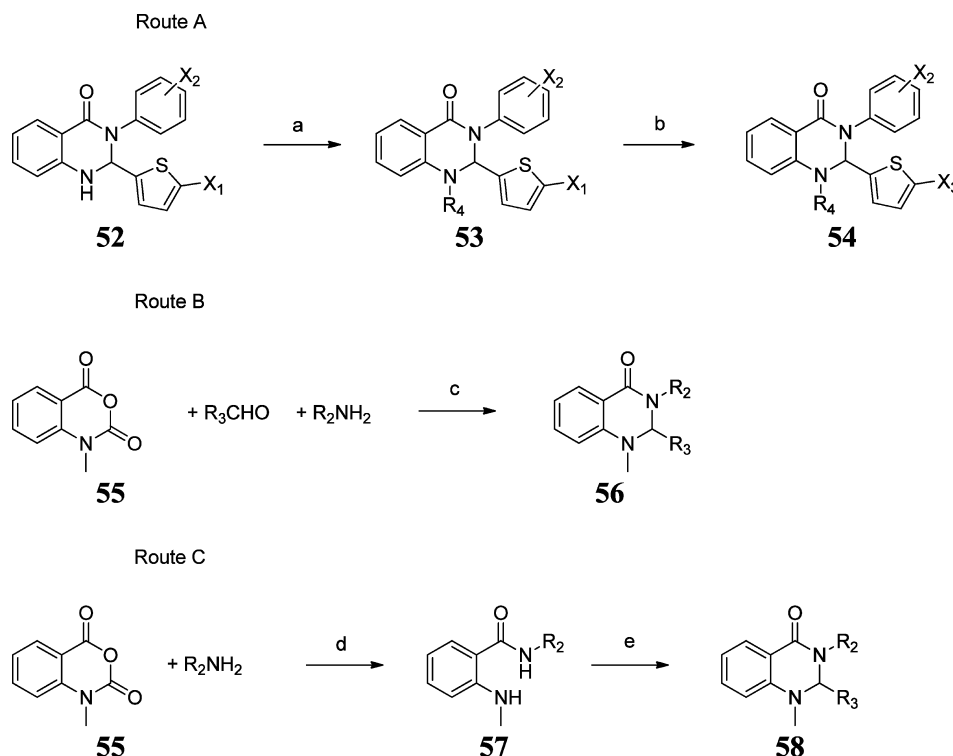
^aSynthesized from commercially available 2-aminobenzanilide. ^bSynthesized according to route B Scheme 2

ound **50**), with introduction of fluorine at C ortho to the amide group being deleterious (compound **51**).

At that stage, we could not exclude that Retro-2^{cycl} could undergo a retrocyclization process to afford imino compounds (although unlikely to occur even in biological media) or more probably an oxidation to compound **7** analogues during storage or tests (as we experienced for numerous analogues). Therefore, alkylated analogues on nitrogen-1 were also prepared and tested.

Three different methods were used for the synthesis of these compounds (Scheme 4). In route A, the NH group of the dihydroquinazolinones previously prepared was alkylated via reaction with sodium hydride or triethylamine and excess halogenated electrophile. The synthesis of **54** analogues consisted of palladium-catalyzed Suzuki coupling¹⁸ of **53** (X₁ = Br) and a commercially available boronic ester, affording **54** in good yields.

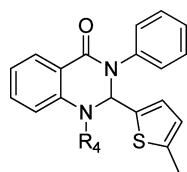
These compounds can be also synthesized via a three-component condensation of an *N*-methyl isatoic anhydride, a primary amine, and an aldehyde in acetic acid at reflux (route B)¹⁹ or via the formation of 2-aminobenzamide derivatives followed by imination/cyclization with aldehydes in THF (route C).

Scheme 4. General Strategy for the Synthesis of N-Protected Dihydroquinazolines^a

^aReagents and conditions. For route A: (a) NaH or NEt₃, R₄X, THF, 0 °C to rt, 16 h; (b) X₁ = Br, X₃B(OR)₂, Pd(PPh₃)₄, K₂CO₃, microwave, DME/H₂O, 110 °C, 1 h. For route B: (c) AcOH, reflux, 4 h. For route C: (d) AcOH, reflux, 4 h; (e) R₃CHO, PTSA, THF, reflux, 16 h.

All compounds synthesized using this synthetic scheme (route A, step a from **1**) and the corresponding protection factors (see Experimental Section) are summarized in Table 4.

Table 4. SAR Exploration of 2-Substituted 1,2,3,4-Dihydroquinazolin-4-one



compd	R ₄	yield (%)	protection factor (%)	EC ₅₀ (μM)
59	<i>t</i> -Boc	84	0	ND
60	COPh	92	0	ND
61	Bn	99	1	ND
62	Me	85	275	10.2
63	Et	85	2.9	ND
64	Pr	73	0	ND
65	<i>n</i> -Bu	74	0	ND

We first protected the dihydroquinazolines with classical protecting groups (*t*-Boc, benzoyl, or benzyl). None of these three compounds were active. Methyl introduction at N1 allowed us to gain active compounds (**62**, EC₅₀ = 10.2 μM), while longer alkyl chains (ethyl **63**, propyl **64**, or butyl **65**) resulted in total loss of activity.

Although the previous variations at the thiophene substituents were not very encouraging, we tested several other derivatives with various substituents at the 5 position, which we

previously identified as the sole possible position for diversity introduction (see Table 5).

Replacement of the methyl group by an ethyl group resulted in slight bioactivity improvement (**66**, EC₅₀ = 4.2 μM). Introduction of a heteroatom (O, N, **67–69**) or a halogen (Cl, **70**) resulted in complete loss of activity.

As previously described in Table 1, 5-thiomethyl, 5-Br enhanced cellular protection against Stx (**71** and **72**, EC₅₀ = 4.8 and 3.4 μM, respectively) whereas the 5-thiophenyl (**73**) and 5-cyano (**74**) led to a decrease and loss of activity, respectively.

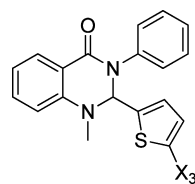
Noteworthy, introduction of a phenyl group (**75**) gave a strong increase of protection (EC₅₀ = 2.1 μM). Conversely, any substitution of this latter group leads to inactive compounds.

Introduction of bicyclic aromatics (1-naphthalene, 2-naphthalene) or heteroaromatics (3-benzothiophene, 5-indole) resulted in inactive compounds. Importantly, introduction of small heteroaromatic groups (2-thiophene, 2-pyridine, 3-furyl) resulted in slightly lower protection values when compared to the parent compound **62**. Unexpectedly, compound **93** showed very weak activity. Finally the best compounds in this series were **90** and **94** with very good EC₅₀ values of 1.5 and 0.3 μM, respectively (see also Table 1).

Since we already demonstrated that the ortho position of the phenyl group at N3 is the sole position (Table 2) to potentially improve protection, we investigated several other functional groups starting from commercially available 2-substituted anilines (Table 6).

At this stage, it is rather difficult to draw a definitive conclusion about the impact of substituents at C2. Nevertheless, we can state that allowed substituents are halogens (Cl **95**, I **96**, F **99**), electron donating groups (OMe **97**, SMe **98**), and even a bulky electron withdrawing group (SO₂Ph **109**).

Table 5. Exploration of Substitution on the Thiophene Ring



Compound	X ₃	Yield (%)	Protection factor (%)	EC ₅₀ (μM)	Compound	X ₃	Yield (%)	Protection factor (%)	EC ₅₀ (μM)
66	Et	44 ^a	323	4.2	85		59 ^a from 72	0	N.D.
67	CHO	84	0	N.D.	86		75 ^a from 72	9.7	N.D.
68	CH ₂ OH	100 ^b from 67	0	N.D.	87		87 ^a from 72	0	N.D.
69	CH ₂ NHBn	72 ^b from 67	6.2	N.D.	88		63 ^a from 72	0	N.D.
70	CH ₂ Cl	33 ^b from 68	0	N.D.	89		78 ^a	94.6	N.D.
71	SMe	60 ^a	265.9	4.8	90		85 ^a	140.4	1.5
72	Br	77 ^a	118	3.4	91		80 ^a from 72	74.7	N.D.
73	SPh	77 ^{a,b}	75.5	N.D.	92		74 ^a	85	N.D.
74	CN	84 ^{a,b}	0	N.D.	93		60 ^b from 72	12	N.D.
75	Ph	60 ^a	309	2.1	94		51 ^a	301	0.3
76	3,4-(OMe) ₂ Ph	75 ^a	1.5	N.D.					
77	3-NO ₂ Ph	77 ^a	0	N.D.					
78	4-CO ₂ MePh	68 ^a	2.9	N.D.					
79	4-COMePh	76 ^a	0.7	N.D.					
80	PhOPh	95 ^a from 72	15.7	N.D.					
81	3,4,5-(OMe) ₃ Ph	73 ^a from 72	0	N.D.					
82	4-(OMe)Ph	70 ^a from 72	26.2	N.D.					
83		76 ^a from 72	0	N.D.					
84	4-CNPh	78 ^a from 72	0	N.D.					

^aSynthesized according to route A, Scheme 4. ^bSee Supporting Information for details.

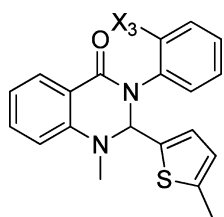
Noteworthy, all dihydroquinazolinones that we synthesized and screened were racemic, so the next step was to individually evaluate the bioactivity of each enantiomer of two of the most potent compounds. For clarity only the data corresponding to **62** are reported herein (see Supporting Information for similar results with compound **94**). A chiral phase separation was performed on a ChiralPak IB HPLC column (see Experimental Section for details). The first eluted compound blocked Stx cytotoxicity (eutomer), while the second eluted compound was inactive (distomer) (Figure 2). Work is currently underway in order to determine the absolute configuration of the eutomers.

To prove that the compounds described herein prevented the deleterious effect of Stx by blocking its intracellular trafficking through the retrograde pathway as reported for Retro-2, we studied the most potent Stx inhibitors using a sulfation assay as previously described.^{11,20} The sulfation assay permits the detection and quantification of STxB retrograde arrival to the TGN. Retrograde transport quantification in the presence of inhibitors (30 μM) is reported in Table 7. 100% means no inhibition at all, whereas 0% indicates a total inhibition of the retrograde transport. These data clearly show that the best compounds (**25**, **66**, and **94**) completely block the retrograde transport of Stx in contrast to the nonoptimized compound Retro-2^{cyd} (**1**).

A large number of trafficking factors have been shown to regulate retrograde transport at the early endosome–TGN interface. However, it has been demonstrated previously that only the SNARE protein syntaxin 5 (and to a lesser extent syntaxins 6 and 16) was strongly relocalized in Retro-2-treated cells, while the subcellular distribution of the Golgi was not affected.¹¹ Thus, we examined whether dihydroquinazolinones also affected the subcellular distribution of the syntaxin 5. The syntaxin 5 (Figure 3, left column) was strongly relocalized in **94**-treated cells after only 30 min of compound treatment (Figure 3, middle panel) as observed after Retro-2^{cyd} (**1**) treatment (Figure 3, lower panel). Moreover, the morphology of the Golgi apparatus was not visibly affected by the dihydroquinazolinone **94** as shown by labeling for the Golgi marker giantin (middle column). These data suggest that dihydroquinazolinones have the same cellular targets as Retro-2, as they both influence localization of syntaxin 5 in the retrograde sorting of Stx.¹¹

Since many pathogens (including viruses and parasites) and bacterial toxins exploit this pathway to traffic within cells, the potent compounds reported here might find broad-spectrum therapeutic use, as exemplified by a recent report demonstrating the protective effect of Retro-2 against *Leishmania*²¹ in addition to toxins¹¹ both in vitro and in vivo. Moreover,

Table 6. SAR Exploration of Ortho Aromatic Ring Substitution at N2



compd	X ₃	yield (%)	protection factor (%)	EC ₅₀ (μM)
95	Cl	67 ^a	230	8.2
96	I	46 ^a	254	5.4
97	OMe	28 ^a	264.4	5.4
98	SMe	73 ^a	150.6	3.8
99	F	51 ^a	208.6	5.5
100	Br	50 ^b	10.5	ND
101	CN	9 ^b	54	ND
102	OPh	60 ^b	23	ND
103	SPh	30 ^b	9.6	ND
104	Ph	64 ^b	99	ND
105	Bn	66 ^b	1	ND
106	CF ₃	16 ^b	3	ND
107	OCF ₃	78 ^b	4.4	ND
108	OBn	62 ^b	9.8	ND
109	SO ₂ Ph	30 ^b	145	8
110	NO ₂	25 ^b	33	ND

^aSynthesized according to route B, Scheme 4. ^bSynthesized according to route C, Scheme 4.

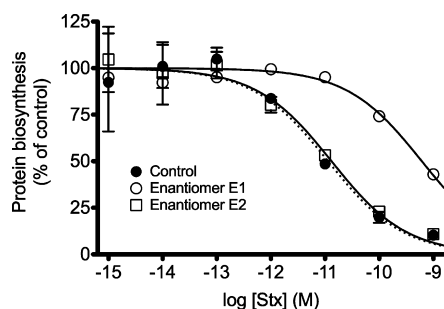


Figure 2. Evaluation of protective activity toward Stx cytotoxicity of each enantiomer of **62** (30 μM). HeLa cells were incubated for 4 h with enantiomer 1 (open circles), enantiomer 2 (open squares, dashed line), or carrier only (DMSO, black-filled circles) before the addition of Stx at the indicated concentrations for 20 h. Medium was removed and replaced with DMEM containing [¹⁴C]leucine at 0.5 μCi/mL for 6 h before counting. Each data point represents the mean of duplicate ± SEM of a representative experiment.

calculated physicochemical properties are encouraging, falling well within the Lipinski rule of five.²² The apparent lipophilicity (cLogP) is rather similar for all compounds and cannot account per se for the observed bioactivity improvement. Altogether, **94** appears as a promising candidate for further development of new therapeutics against Stx.

CONCLUSION

Optimization of the three main moieties of Retro-2^{cycl} allowed us to identify a dihydroquinazolinone derivative that is a potent inhibitor of Shiga toxin, with EC₅₀ = 300 nM. We demonstrate that the mode of action of this compound is similar to that of Retro-2, acting by selective inhibition of the retrograde

Table 7. Retrograde Transport Inhibition of Stx by Dihydroquinazolinones Derivatives and Calculated Physicochemical Properties

compd	retrograde transport (% control)	EC ₅₀ (μM)	MW	H-bond donor	H-bond acceptor	cLogP
DMSO	100					
1	36.9	27.3	320	1	2	3.67
17	13.5	8.7	334	1	2	4.2
25	0	1.4	403	1	3	3.97
62	38.7	10.2	334	0	2	4.49
66	0	4.2	348	0	2	5.02
94	0	0.3	417	0	3	4.8

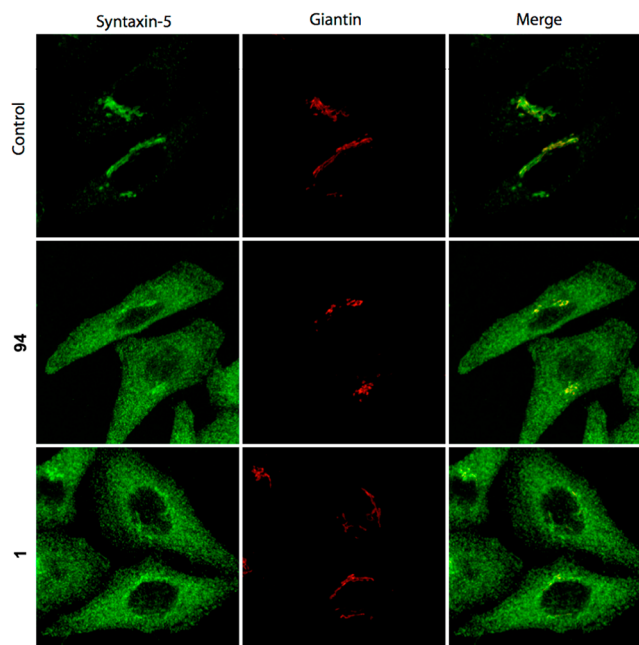


Figure 3. Dihydroquinazolinones relocalize the SNARE protein syntaxin 5. Cells were treated for 30 min with carrier (DMSO, upper panel), **94** (middle panel), or **1** (lower panel) at 20 μM, fixed, and labeled for the indicated proteins.

transport. We also show that only one enantiomer is active. The other has no effect on Stx cytotoxicity. As a result, we illustrate that compounds described herein specifically impact a protein implicated in the retrograde transport of Stx. The low molecular weight, simple structure inhibitors we found represent an attractive starting point for the potential development of dihydroquinazolinone drugs against Stx-associated diseases. Further biological investigations, including in vitro ADME, toxicity, and pharmacokinetic studies in vivo, are currently underway to establish their druglike properties.

EXPERIMENTAL SECTION

Synthesis. All chemicals and solvents used in the synthesis were reagent grade and were used without additional purification. THF and CH₂Cl₂ were distilled, respectively, from sodium/benzophenone ketyl and calcium hydride before use. Glassware was flame-dried under vacuum and cooled under nitrogen to room temperature. All reactions were performed under dry nitrogen gas and monitored by thin-layer chromatography (TLC). TLC was performed with precoated TLC silica gel 60 F254, and organic compounds were visualized by UV light (254 nm), iodine vapor, and phosphomolybdic acid [10% (w/v) in ethanol] staining with heating.

The large-scale purification was performed on a CombiFlash with a UV-vis detector with RediSep columns. The samples were adsorbed on Celite or silica and loaded into solid load cartridges. An ethyl acetate/cyclohexane or methanol/methylene chloride gradient was employed. Fractions were collected based on detection at 254 nm.

The purity of the tested compounds was determined by LC/MS (UV detection) using two distinct elution conditions (see below) and was higher than 95%.

HPLC-MS analysis and purification were performed using a Waters system (2525 binary gradient module, in-line degasser, 2767 sample manager, 2996 photodiode array detector) with a binary gradient solvent delivery system. This system was coupled with a Waters Micromass ZQ system with a ZQ2000 quadrupole analyzer. The ionization was performed by electrospray, and the other parameters were as follows: source temperature 120 °C, cone voltage 20 V, and continuous sample injection at 0.3 mL/min flow rate. Mass spectra were recorded in both positive and negative ion modes in the m/z 100–2000 range and treated with the Mass Lynx 4.1 software.

The eluent was a gradient of 99.9% water/0.1% HCOOH and 99.9% MeCN/0.1% HCOOH or 99.9% water/0.1% HCOOH and 99.9% MeOH/0.1% HCOOH. Each compound was applied to a 100 mm × 4.6 mm (5 μ m) WATERS XBridge C18 column equilibrated with H₂O/MeCN or H₂O/MeOH 95:5. The following gradients were the following:

Gradient A: Samples were eluted by increasing MeOH to 100% (25 min), then staying at 100% (5 min).

Gradient B: Samples were eluted by increasing MeOH to 90% (24 min), then to 100% (1 min), and staying at 100% (5 min).

Gradient C: Samples were eluted by increasing MeOH to 80% (24 min), then to 100% (1 min), and staying at 100% (5 min).

Gradient D: Samples were eluted by increasing MeCN to 100% (25 min), then staying at 100% (1 min).

Gradient E: Samples were eluted by increasing MeCN to 90% (24 min), then to 100% (1 min), and staying at 100% (5 min).

Gradient F: Samples were eluted by increasing MeCN to 80% (24 min), then 100% (1 min) and stay at 100% (5 min).

Gradient G: Samples were eluted by increasing MeCN to 60% (24 min), then to 100% (1 min), and staying at 100% (5 min).

HPLC (chiral) analyses were performed on a system equipped with a binary gradient solvent delivery system (LC-20AB, Shimadzu), a SIL-20A autosampler (Shimadzu), and a photodiode array detector (SPD-20A, Shimadzu).

NMR experiments were performed on a Bruker Avance 400 Ultrashield spectrometer. ¹H NMR and ¹³C spectra were recorded at room temperature at 400 and 100 MHz, respectively, samples were dissolved in DMSO-*d*₆ at a concentration of approximately 5 mM. The DMSO singlet signal was set up at 2.50 ppm. Chemical shifts are given in ppm and the coupling constants in Hz. Spectral data are consistent with assigned structures.

Physicochemical properties were calculated using MarvinSketch 5.4.1.1 software (ChemAxon).

High-resolution mass spectrometry (HRMS) was performed using the Imagif platform (CNRS, Gif-sur-Yvette, France), and results were recorded on a ESI/TOF LCP premier XE mass spectrometer (Waters) using flow injection analysis mode.

2-(5-Ethylthiophen-2-yl)-3-phenyl-2,3-dihydroquinazolin-4(1H)-one (17). To a solution of 2-aminobenzanilide (212 mg, 1.0 mmol) in methanol (0.2 M) was added 5-ethylthiophen-2-carboxaldehyde (125 μ L, 1.0 mmol), and the solution was stirred at room temperature until complete consumption of starting materials. The precipitate was filtered to give the title compound (147 mg, 52%) as a beige solid. ¹H NMR (400 MHz, DMSO-*d*₆) δ (ppm) = 1.13 (t, *J* = 7.6 Hz, 3H), 2.67 (q, *J* = 7.6 Hz, 2H), 6.42 (d, *J* = 2.4 Hz, 1H), 6.58 (d, *J* = 3.2 Hz, 1H), 6.74–6.83 (m, 3H), 7.24 (t, *J* = 7.2 Hz, 1H), 7.30–7.40 (m, 5H), 6.64 (d, *J* = 2.8 Hz, 1H), 7.73 (d, *J* = 7.2 Hz, 1H). ¹³C NMR (100 MHz, DMSO-*d*₆) δ (ppm) = 15.5, 22.6, 69.6, 115.1, 115.4, 117.9, 122.6, 126.0, 126.2, 126.3, 127.9, 128.6, 133.7, 140.4, 141.6, 146.2, 146.6, 161.4. MS (ESI) [M + H]⁺ = 335.1. LC/MS (X-bridge 100 mm × 4.6 mm): *t*_R = 7.57 min, m/z 335.1 ([M + H]⁺).

2-(5-(2-Methylthiazol-4-yl)thiophen-2-yl)-3-phenyl-2,3-dihydroquinazolin-4(1H)-one (25). To a solution of 2-aminobenzanilide (212 mg, 1.0 mmol) in methanol (0.3 M) was added 5-(2-methyl-3-thiazol-4-yl)-2-thiophenecarbaldehyde (209 mg, 1.0 mmol), and the solution was stirred at room temperature for 24 h. The precipitate was filtered and washed with a small quantity of MeOH to give the imino compound (252 mg, 62%) as a yellow solid. To a mixture of NaH in anhydrous THF (0.5 mL) was added dropwise a solution of the imino compound in anhydrous THF (1.1 mL) at 0 °C. After 1 h at 0 °C, the reaction was quenched with a saturated solution of NaHCO₃ (1 mL). The mixture was partitioned between a saturated solution of NaHCO₃ (10 mL) and CH₂Cl₂ (10 mL). The aqueous layer was extracted with CH₂Cl₂ (2 × 10 mL). The combined organic layers were washed with brine (10 mL), dried over anhydrous MgSO₄, filtered, and concentrated in vacuum. The purification by silica gel chromatography (ethyl acetate/cyclohexane, 1/1) yielded the expected compound 25 (34 mg, 68%) as a yellow solid. ¹H NMR (400 MHz, CDCl₃) δ (ppm) = 2.67 (s, 3H), 6.20 (s, 1H), 6.65 (d, *J* = 8.1 Hz, 1H), 6.78 (d, *J* = 3.8 Hz, 1H), 6.85–6.91 (m, 1H), 7.06 (s, 1H), 7.08 (d, *J* = 3.8 Hz, 1H), 7.18–7.24 (m, 1H), 7.26–7.33 (m, 5H), 8.00 (dd, *J* = 7.8 Hz, *J*' = 1.6 Hz, 1H). ¹³C NMR (100 MHz, CDCl₃) δ (ppm) = 19.2, 70.9, 111.8, 115.7, 117.1, 120.0, 123.1, 126.8, 127.0, 127.3, 129.0, 129.1, 134.0, 138.6, 140.5, 143.4, 145.0, 148.9, 162.5, 166.4. MS (ESI) [M + H]⁺ = 404.0. LC/MS (X-bridge 100 mm × 4.6 mm): *t*_R = 7.98 min, m/z 404.0 ([M + H]⁺).

1-Methyl-2-(5-methylthiophen-2-yl)-3-phenyl-2,3-dihydroquinazolin-4(1H)-one (62). To a mixture of NaH (19 mg, 0.475 mmol) in anhydrous THF (0.3 M) was added dropwise a solution of 1 (100 mg, 0.312 mmol) in anhydrous THF (0.5M) at 0 °C. After 30 min, iodomethane (21 μ L, 0.337 mmol) was added dropwise. After 10 min, the solution was warmed to room temperature and stirred for 3 h. The reaction was then quenched with a saturated solution of NaHCO₃. The aqueous layer was then repeatedly extracted with CH₂Cl₂. The combined organic layers were then washed with a 1 M solution of HCl (2 × 10 mL), dried over anhydrous Na₂SO₄, filtered, and concentrated in vacuum. The purification by silica gel chromatography (ethyl acetate/cyclohexane, 3/7) of the crude mixture yielded the expected compound (89 mg, 85%) as a white solid. ¹H NMR (400 MHz, DMSO) δ (ppm) = 2.34 (s, 3H), 2.93 (s, 3H), 5.91 (s, 1H), 6.50 (d, *J* = 2.4 Hz, 1H), 6.64–6.67 (m, 2H), 6.96 (t, *J* = 7.6 Hz, 1H), 7.25–7.39 (m, 5H), 7.42–7.47 (m, 1H), 8.11 (dd, *J* = 1.6 Hz, *J*' = 7.6 Hz, 1H). ¹³C NMR (100 MHz, DMSO) δ (ppm) = 15.2, 35.9, 77.9, 112.8, 117.5, 119.0, 124.0, 126.6, 126.7, 126.9, 128.9, 128.9, 134.0, 137.0, 140.3, 140.5, 146.3, 161.8. MS (ESI) [M + H]⁺ = 334.9. LC/MS (X-bridge 100 mm × 4.6 mm): *t*_R = 8.20 min, m/z 334.9 ([M + H]⁺). Gradient A: *t*_R = 21.15 min. Gradient D: *t*_R = 17.99 min. IR (neat, cm⁻¹) 3063, 2915, 2856, 1670, 1608, 1531, 1468, 1226, 761, 693. HRMS m/z [(M + H)⁺] calcd for C₂₀H₁₉N₂O₂S 335.1204, found 335.1218.

2-(5-Ethylthiophen-2-yl)-1-methyl-3-phenyl-2,3-dihydroquinazolin-4(1H)-one (66). To a mixture of NaH (15 mg, 0.375 mmol) in anhydrous THF (0.3 M) was added dropwise a solution of 17 (100 mg, 0.299 mmol) in anhydrous THF (0.5 M) at 0 °C. After 30 min, iodomethane (20 μ L, 0.321 mmol) was added dropwise. After 10 min, the solution was warmed to room temperature and stirred for 3 h. The reaction was then quenched with a saturated solution of NaHCO₃. The aqueous layer was then repeatedly extracted with CH₂Cl₂. The combined organic layers were then washed with a 1 M solution of HCl (2 × 10 mL), dried over anhydrous Na₂SO₄, filtered, and concentrated in vacuum. The purification by silica gel chromatography (ethyl acetate/cyclohexane, 3/7) of the crude mixture yielded the expected compound (87 mg, 84%) as a white solid. ¹H NMR (400 MHz, CDCl₃) δ (ppm) = 1.21 (t, *J* = 7.5 Hz, 3H), 2.70 (q, *J* = 7.5 Hz, 2H), 2.94 (s, 3H), 5.92 (s, 1H), 6.51–6.54 (m, 1H), 6.65–6.68 (m, 2H), 6.95 (t, *J* = 8.1 Hz, 1H), 7.24–7.47 (m, 6H), 8.10 (dd, *J* = 7.7 Hz, *J*' = 1.6 Hz, 1H). ¹³C NMR (100 MHz, CDCl₃) δ (ppm) = 15.5, 23.4, 36.2, 78.2, 113.0, 117.7, 119.2, 122.3, 126.7, 126.8, 127.1, 129.1, 129.2, 134.2, 136.9, 140.7, 146.5, 162.0. MS (ESI) [M + H]⁺ = 349.1. LC/MS (X-bridge 100 mm × 4.6 mm): *t*_R = 8.77 min, m/z 349.1 ([M + H]⁺). Gradient A: *t*_R = 21.95 min. Gradient D: *t*_R = 19.02 min. IR (neat,

cm⁻¹) 3068, 2968, 2863, 1655, 1605, 1495, 749, 694. HRMS *m/z* [(M + H)⁺] calcd for C₂₁H₂₁N₂O₅ 349.1373, found 349.1373.

1-Methyl-2-(5-(2-methylthiazol-4-yl)thiophen-2-yl)-3-phenyl-2,3-dihydroquinazolin-4(1H)-one (94). To a mixture of NaH (19 mg, 0.475 mmol) in anhydrous THF (0.3 M) was added dropwise a solution of 25 (100 mg, 0.248 mmol) in anhydrous THF (0.5 M) at 0 °C. After 30 min, iodomethane (17 μL, 0.273 mmol) was added dropwise. After 10 min, the solution was warmed to room temperature and stirred for 3 h. The reaction was then quenched with a saturated solution of NaHCO₃. The aqueous layer was then repeatedly extracted with CH₂Cl₂. The combined organic layers were then washed with a 1 M solution of HCl (2 × 10 mL), dried over anhydrous Na₂SO₄, filtered, and concentrated in vacuum. The purification by silica gel chromatography (ethyl acetate/cyclohexane, 2/8) of the crude mixture yielded the expected compound (86 mg, 83%) as a white solid. ¹H NMR (400 MHz, CDCl₃) δ (ppm) = 2.70 (s, 3H), 2.99 (s, 3H), 5.98 (s, 1H), 6.66 (d, *J* = 8.1 Hz, 1H), 6.81 (d, *J* = 3.8 Hz, 1H), 6.92–6.99 (m, 1H), 7.09 (s, 1H), 7.17 (d, *J* = 3.8 Hz, 1H), 7.24–7.39 (m, 5H), 7.40–7.46 (m, 1H), 8.10 (dd, *J* = 7.8 Hz, *J'* = 1.6 Hz, 1H). ¹³C NMR (100 MHz, CDCl₃) δ (ppm) = 19.3, 36.4, 78.1, 111.9, 113.3, 117.8, 119.5, 123.2, 126.8, 127.3, 127.6, 129.3, 129.4, 134.3, 138.6, 139.4, 140.6, 146.3, 148.8, 162.0, 166.5. MS (ESI) [M + H]⁺ = 417.8. LC/MS (X-bridge 100 mm × 4.6 mm): *t*_R = 8.68 min, *m/z* 417.8 [(M + H)⁺]. Gradient A: *t*_R = 20.92 min. Gradient D: *t*_R = 17.87 min. IR (neat, cm⁻¹) 3075, 2958, 2871, 1651, 1605, 1494, 749, 696. HRMS *m/z* [(M + H)⁺] calcd for C₂₃H₂₀N₃O₅ 418.1048, found 418.1048.

Chemicals for in Vitro Experiments. The following products were purchased from the indicated commercial sources: [³⁵S]-methionine and [¹⁴C]leucine (Perkin-Elmer), Shiga-like toxin 1 (Stx, List Biological Laboratories, Inc.), DMSO (Sigma), fetal bovine serum (Sigma), glutamine, pyruvate, nonessential amino acids, and antibiotics solutions (Gibco). STxB-Sulf₂ and anti-STxB mAb 13C4 were prepared as previously described.^{20,23}

Intoxication Assays. HeLa cells were maintained at 37 °C under 5% CO₂ in DMEM (Dulbecco's modified Eagle medium, Invitrogen), supplemented with 10% fetal bovine serum, 4.5 g/L glucose, 100 U/mL penicillin, 100 μg/mL streptomycin, 4 mM glutamine, 5 mM pyruvate. The cells were plated at a density of 50 000 cells per well in 96-well Cytostar-T scintillating microplates (Perkin-Elmer) with scintillator incorporated into the polystyrene plastic. After incubation with either 30 μM or various concentrations of compounds (or 0.1% DMSO) for 4 h at 37 °C, cells were challenged with increasing doses of Stx in the continued presence of compounds. After incubation for 20 h, the medium was removed and replaced with DMEM without leucine (Eurobio) containing 10% fetal bovine serum, 2 mM L-glutamine, 0.1 mM nonessential amino acids, 1% penicillin/streptomycin supplemented with 0.5 μCi/mL [¹⁴C]leucine. The cells were grown for an additional 6 h at 37 °C in an atmosphere of 5% CO₂ and 95% air. Protein biosynthesis was then determined by measuring the incorporation of radiolabeled leucine into cells using a Wallac 1450 MicroBeta liquid scintillation counter (Perkin-Elmer).

The mean percentage of protein biosynthesis was determined and normalized from duplicate wells. All values are expressed as the mean ± SEM. Data were fitted with Prism, version 5, software (Graphpad Inc., San Diego, CA) to obtain the 50% inhibitory toxin concentration (IC₅₀), i.e., the concentration of toxin that is required to kill 50% of cells. IC₅₀ values and protection factor *R* (*R* = IC₅₀(drug)/IC₅₀(DMSO)) were determined by the software's nonlinear regression "dose–response EC₅₀ shift equation". The goodness of fit for Stx alone (carrier) or with drug was assessed by *r*² and confidence intervals. The percentage of cell protection was calculated for each compound after determination of the *R* value (*R*_{drug}) and compared to the *R* value of Retro-2 (*R*_{ref}):

$$\% \text{ protection} = \frac{R_{\text{drug}} - 1}{R_{\text{ref}} - 1} \times 100$$

All compounds were tested at 30 μM, and Retro-2 compound equals 100% protection at 30 μM.

Determination of EC₅₀ Values of Dihydroquinazolinones.

For compounds that displayed a percentage of protection equal or superior to 100%, the EC₅₀ represents the concentration giving 50% of its full inhibitory effect against Stx. EC₅₀ was used to compare the efficacy of compounds because it is more precise than *R* values and associated % protection. This is due to the fact that *R* values may fluctuate between cell experiments from different 96-wells plates corresponding to compounds tested on different days. In contrast the EC₅₀ value for a single compound is calculated from experimental data obtained on a single 96-well plate. Cell assays were performed with various concentrations of the inhibitor. For each concentration, a percentage of protection was determined from *R* values calculated with Prism software with *R*_{max} corresponding to the higher value of *R* of the series:

$$\% \text{ protection} = \frac{R - 1}{R_{\text{max}} - 1} \times 100$$

Drug concentration was plotted against the corresponding percentage of protection of cells, and the 50% efficacy concentration (EC₅₀) was calculated by nonlinear regression using the Prism software package.

Sulfation Assay. The sulfation assay was performed as previously described.^{20,24,25} Briefly, a STxB variant termed STxB-Sulf₂ that bears a tandem of protein sulfation recognition sites was bound to cells on ice. After washing, the cells were incubated for 20 min at 37 °C in the presence of [³⁵S]sulfate, STxB was immunoprecipitated, and sulfation was quantified by autoradiography.

Immunofluorescent Staining. For immunofluorescence experiments, compound-treated HeLa cells were incubated for 30 min in the continued presence of compounds (20 μM). Cells were fixed and immunolabeled with antibodies corresponding to the indicated proteins. Samples were imaged on a Ti inverted microscope (Nikon) fitted with a confocal A1R system, using a 60× oil immersion objective, NA 1.4. NIS Elements, MetaMorph (Molecular Devices), and ImageJ (National Institutes of Health, Bethesda, MD) software was used for image processing. Maximum projections of six to eight optical Z slices (250 nm Z separation) are shown. Antibody against syntaxin 5 was commercially purchased from Synaptic Systems. Antibody against gintin was from BD Biosciences.

■ ASSOCIATED CONTENT

Supporting Information

Synthetic procedures and compound characterization and biological assays. This material is available free of charge via the Internet at <http://pubs.acs.org>.

■ AUTHOR INFORMATION

Corresponding Author

*For D.G.: phone, + 33 1 69 08 76 46; fax, + 33 1 69 08 90 71; e-mail, daniel.gillet@cea.fr. For J.-C.C.: phone, + 33 1 69 08 21 07; fax, + 33 1 69 08 79 91; e-mail, jean-christophe.cintrat@cea.fr.

Notes

The authors declare no competing financial interest.

■ ACKNOWLEDGMENTS

This work (Project RetroScreen) has been funded by the French National Agency for Research (ANR) under Contract ANR-11-BSV2-0018 and by CEA.

■ ABBREVIATIONS USED

Retro-2^{cycl}, cyclized Retro-2; Stx, Shiga toxin; HUS, hemolytic uremic syndrome; STEC, Stx-producing *E. coli*; EHEC, enterohemorrhagic *E. coli*; Gb3, globotriaosylceramid; STxA, A-subunit of Shiga toxin; STxB, B-subunit of Shiga toxin; ER, endoplasmic reticulum; TGN, trans Golgi network

■ REFERENCES

- (1) Acheson, D. W. K.; Keusch, G. T. The Family of Shiga Toxins. In *The Comprehensive Sourcebook of Bacterial Protein Toxins*, 2nd ed.; Alouf, J. E., Freer, J. H., Eds.; Elsevier: Paris, 1999; pp 229–242.
- (2) O'Brien, A. D.; Holmes, R. K. Shiga and Shiga-like toxins. *Microbiol. Rev.* **1987**, *51*, 206–220.
- (3) Tarr, P. I.; Gordon, C. A.; Chandler, W. L. Shiga-toxin-producing *Escherichia coli* and haemolytic uraemic syndrome. *Lancet* **2005**, *365*, 1073–1086.
- (4) Karch, H.; Denamur, E.; Dobrindt, U.; Finlay, B. B.; Hengge, R.; Johannes, L.; Ron, E. Z.; Tønjum, T.; Sansonetti, P. J.; Vicente, M. The enemy within us: lessons from the 2011 European *Escherichia coli* O104:H4 outbreak. *EMBO Mol. Med.* **2012**, *4*, 841–848.
- (5) Sandvig, K.; Spilsberg, B.; Lauvrak, S. U.; Torgersen, M. L.; Iversen, T. G.; van Deurs, B. Pathways followed by protein toxins into cells. *Int. J. Med. Microbiol.* **2004**, *293*, 483–490.
- (6) Johannes, L.; Popoff, V. Tracing the retrograde route in protein trafficking. *Cell* **2008**, *135*, 1175–1187.
- (7) Tarr, P. I.; Sadler, J. E.; Chandler, W. L.; George, J. N.; Tsai, H. M. Should all adult patients with diarrhoea-associated HUS receive plasma exchange? *Lancet* **2012**, *379*, 516 ; author reply 516–517.
- (8) Menne, J.; Nitschke, M.; Stingle, R.; Abu-Tair, M.; Beneke, J.; Bramstedt, J.; Bremer, J. P.; Brunkhorst, R.; Busch, V.; Dengler, R.; Deuschl, G.; Fellermann, K.; Fickenscher, H.; Gerigk, C.; Goettsche, A.; Greeve, J.; Hafer, C.; Hagenmuller, F.; Haller, H.; Herget-Rosenthal, S.; Hertenstein, B.; Hofmann, C.; Lang, M.; Kielstein, J. T.; Klostermeier, U. C.; Knobloch, J.; Kuehbacher, M.; Kunzendorf, U.; Lehnert, H.; Manns, M. P.; Menne, T. F.; Meyer, T. N.; Michael, C.; Munte, T.; Neumann-Grutzeck, C.; Nuernberger, J.; Pavenstaedt, H.; Ramazan, L.; Renders, L.; Repenthin, J.; Ries, W.; Rohr, A.; Rump, L. C.; Samuelsson, O.; Sayk, F.; Schmidt, B. M.; Schnatter, S.; Schockmann, H.; Schreiber, S.; von Seydewitz, C. U.; Steinhoff, J.; Stracke, S.; Suerbaum, S.; van de Loo, A.; Vischedyk, M.; Weissenborn, K.; Wellhoner, P.; Wiesner, M.; Zeissig, S.; Buning, J.; Schiffer, M.; Kuehbacher, T. Validation of treatment strategies for enterohaemorrhagic *Escherichia coli* O104:H4 induced haemolytic uraemic syndrome: case-control study. *BMJ* **2012**, *345*, e4565.
- (9) Lapeyraque, A. L.; Malina, M.; Fremeaux-Bacchi, V.; Boppel, T.; Kirschfink, M.; Oualha, M.; Proulx, F.; Clermont, M. J.; Le Deist, F.; Niaudet, P.; Schaefer, F. Eculizumab in severe Shiga-toxin-associated HUS. *N. Engl. J. Med.* **2011**, *364*, 2561–2563.
- (10) Saenz, J. B.; Doggett, T. A.; Haslam, D. B. Identification and characterization of small molecules that inhibit intracellular toxin transport. *Infect. Immun.* **2007**, *75*, 4552–4561.
- (11) Stechmann, B.; Bai, S. K.; Gobbo, E.; Lopez, R.; Merer, G.; Pinchard, S.; Panigai, L.; Tenza, D.; Raposo, G.; Beaumelle, B.; Sauvage, D.; Gillet, D.; Johannes, L.; Barbier, J. Inhibition of retrograde transport protects mice from lethal ricin challenge. *Cell* **2010**, *141*, 231–242.
- (12) Wahome, P. G.; Bai, Y.; Neal, L. M.; Robertus, J. D.; Mantis, N. J. Identification of small-molecule inhibitors of ricin and shiga toxin using a cell-based high-throughput screen. *Toxicol.* **2010**, *56*, 313–323.
- (13) Barbier, J.; Bouclier, C.; Johannes, L.; Gillet, D. Inhibitors of the cellular trafficking of ricin. *Toxins (Basel, Switz.)* **2012**, *4*, 15–27.
- (14) Mukhopadhyay, S.; Linstedt, A. D. Manganese blocks intracellular trafficking of Shiga toxin and protects against Shiga toxicosis. *Science* **2012**, *335*, 332–335.
- (15) Park, J. G.; Kahn, J. N.; Tumer, N. E.; Pang, Y. P. Chemical structure of Retro-2, a compound that protects cells against ribosome-inactivating proteins. *Sci. Rep.* **2012**, *2*, 631.
- (16) Hamuro, Y.; Geib, S. J.; Hamilton, A. D. Oligoantranilamides. Non-peptide subunits that show formation of specific secondary structure. *J. Am. Chem. Soc.* **1996**, *118*, 7529–7541.
- (17) Prakash, M.; Kesavan, V. Highly enantioselective synthesis of 2,3-dihydroquinazolinones through intramolecular amidation of imines. *Org. Lett.* **2012**, *14*, 1896–1899.
- (18) Miyaura, N.; Suzuki, A. Palladium-catalyzed cross-coupling reactions of organoboron compounds. *Chem. Rev.* **1995**, *95*, 2457–2483.
- (19) Surpur, M. P.; Singh, P. R.; Patil, S. B.; Samant, S. D. Expedient one-pot and solvent-free synthesis of dihydroquinazolin-4(1H)-ones in the presence of microwaves. *Synth. Commun.* **2007**, *37*, 1965–1970.
- (20) Amessou, M.; Popoff, V.; Yelamos, B.; Saint-Pol, A.; Johannes, L. Measuring Retrograde Transport to the Trans-Golgi Network. In *Current Protocols in Cell Biology*; Wiley: Somerset, NJ, 2006.
- (21) Canton, J.; Kima, P. E. Targeting host syntaxin-5 preferentially blocks *Leishmania* parasitophorous vacuole development in infected cells and limits experimental *Leishmania* infections. *Am. J. Pathol.* **2012**, *181*, 1348–1355.
- (22) Lipinski, C. A.; Lombardo, F.; Dominy, B. W.; Feeney, P. J. Experimental and computational approaches to estimate solubility and permeability in drug discovery and development settings. *Adv. Drug Delivery Rev.* **1997**, *23*, 3–25.
- (23) Mallard, F.; Antony, C.; Tenza, D.; Salamero, J.; Goud, B.; Johannes, L. Direct pathway from early/recycling endosomes to the Golgi apparatus revealed through the study of shiga toxin B-fragment transport. *J. Cell Biol.* **1998**, *143*, 973–990.
- (24) Johannes, L.; Tenza, D.; Antony, C.; Goud, B. Retrograde transport of KDEL-bearing B-fragment of Shiga toxin. *J. Biol. Chem.* **1997**, *272*, 19554–19561.
- (25) Mallard, F.; Johannes, L. Shiga toxin B-subunit as a tool to study retrograde transport. *Methods Mol. Med.* **2003**, *73*, 209–220.